MPPT-PWM - A Maximum Power Point Tracking (MPPT) Strategy Using Variable Speed Wind Turbines (VSWTs)

Thiagarajan Yogamoorthi[1](✉), Gabriel Gomes de Oliveira[2], Vania Vieira Estrela[3], Henrique Rego Monteiro da Hora[4], Abdeldjalil Khelassi[5], Nikolaos Andreopoulos[3], Maria Aparecida de Jesus[3], and Yuzo Iano[2]

[1] Sri Venkateshwaraa College of Engineering and Technology, Puducherry, India
[2] State University of Campinas, São Paulo, Brazil
yuzo@decom.fee.unicamp.br
[3] Federal Fluminense University, Rio de Janeiro, Brazil
vania.estrela.phd@ieee.org
[4] Instituto Federal Fluminense, Campus dos Goytacazes, Rio de Janeiro, Brazil
[5] Abou Bakr Belkaid University of Tlemcen, Tlemcen, Algeria

Abstract. Nowadays, wind generators can supply more electric energy for standalone and grid-connected applications. This investigative work emphasizes a new optimal control method design to achieve the Maximum Power Point Tracking (MPPT) using Variable Speed Wind Turbines (VSWTs) termed MPPT-PWM. The VSWT output is initially coupled with a Permanent Magnet Synchronous Generator (PMSG) to transform wind energy to a fixed DC level using a chopper. Later, DC output from the chopper is inverted to obtain AC power using the PWM technique for adequate power flow. Experiments ratify the remarkable performance of the MPPT-PWM framework.

Keywords: Variable Speed Wind Turbines (VSWTs) · Maximum Power Point Tracking (MPPT) · Permanent Magnet Synchronous Generator (PMSG) · Direct Current (DC) · Alternating Current (AC) · Pulse Width Modulation (PWM) · Horizontal Axis Wind Turbine (HAWT) · Distributed Generation (DG)

1 Introduction

Global warming has augmented the atmospheric gas concentration produced by fossil fuel burning [1]. Many energy-related issues, e.g., exhausting fossil-fuel reserves, security concerns, and global warming, intensify the need for renewable energy. All over the world, electric power generation via non-conventional sources receives considerable attention owing to the depletion of fossil fuels and other environmental issues [2–6]. Their main advantages are pollution-free and inexhaustible, while the main shortcomings are the cost and uncontrollability. The eolic turbines can harness wind and transform this ample resource into electricity by generators. For the most part, wind power hinges on

Y. Iano et al. (Eds.): BTSym 2020, SIST 233, pp. 1016–1026, 2021.
https://doi.org/10.1007/978-3-030-75680-2_109

geographic and weather conditions that vary from time-to-time. Wind power production is cost-competitive because of three reasons:

1. The state incentives;
2. The wind manufacturing industry has upgraded the aerodynamic efficiency of the eolic turbine;
3. The power semiconductors evolution and new control methodology for the variable-speed wind turbine permit the optimization of eolic turbine performance.

Wind supplies kinetic energy, which is pollution-free, cost-competitive, infinitely sustainable, and one of the fastest-growing renewable energy sources globally. It does not yield greenhouse gases or toxic radioactive waste. The wind allows the rotation of fast-moving wings that exert a torque on the rotor. The bladed rotor is the most fundamental and noticeable part of the wind turbine. Eolic turbines can be twofold contingent on the blade positions:

1. Based on the axis of rotation:

   – Vertical Axis Wind Turbine (VAWT);
   – Horizontal Axis Wind Turbine (HAWT).

2. Regarding the operation speed:

   – Constant speed;
   – Variable rate.

Earlier, the cost and variations of wind energy made it scarcely used. However, recent technological improvements have reduced the price by increasing the Wind Energy Conversion System (WECS) throughput. Consequently, the variable speed WECS encounters several applications, e.g., water pumping systems, standalone schemes for homes/businesses, telecommunications, radar activation, navigational aids, weather stations/seismic monitoring, and air-traffic control, to refer to a few.

The present article follows this structure: Sect. 2 discourses about the Maximum Power Point Tracking (MPPT) scheme via Variable Speed Wind Turbines (VSWTS) named MPPT-PWM. Results and a technical discussion appear in Sect. 3. Section 4 wraps up this manuscript with conclusions.

2 Development

The rotor revolves around a shaft to convey the nacelle's motion (which is the massive housing portion at the wind turbine tower top), as in Fig. 1. The slowly rotating shaft connects to a gearbox within the nacelle to expressively augment the rotational shaft velocity. The high-speed shaft output connected to the generator converts the rotation into electricity at medium voltage (about a few hundred volts) [7–11]. Wind power production happens twofold: (i) constant speed and (ii) variable speed through power electronic converters. Inconsistent speed power production is attractive for a wind turbine because it attains maximum efficiency at all wind speeds.

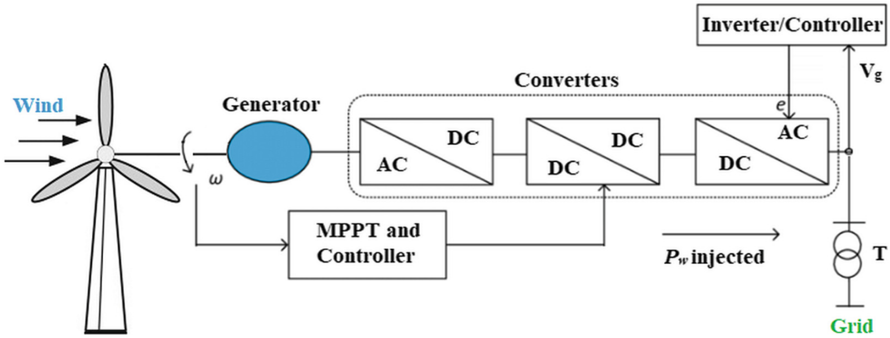

Fig. 1. MPPT scheme

2.1 MPPT for a WECS

The electrical energy needs with fossil fuel scarcity, demand, and indispensable deploying a distributed generation (DG) structure to satisfy local demands where renewable energy sources play a unique role [12–15]. This manuscript proposes and develops an optimal control method to bring out electricity uninterruptedly through variable speed wind turbines (VSWTS). For a VSWT coupled with a Permanent Magnet Synchronous Generator (PMSG), the initial stage converts the output to a fixed DC using a chopper. Subsequently, inverting the DC output from the chopper creates AC via the PWM technique.

2.2 Mathematical Model of the VSWT

Wind turbines convert the eolic kinetic energy E_c into electrical energy utilizing power converters. The energy obtained from conversion mainly hinges on the wind speed as well as the swept area of the turbine. The wind kinetic energy is:

$$E_c = mV^2/2 \tag{1}$$

The rate of energy change yields wind power as follows:

$$P_w = dE_c/dt = V^2[dm/dt]/2 \tag{2}$$

Then, the mass flow rate is given as:

$$dm/dt = \rho AV \tag{3}$$

Substituting (3) in (2) yields:

$$P_w = \left(\rho AV^3\right)/2 \tag{4}$$

The power coefficient becomes:

$$C_p = P_m/P_w \tag{5}$$

Where $C_p < 1$. From the two previous expressions, the wind output power turns into:

$$P_m = \left(\rho A V^3 C_p\right)/2 \tag{6}$$

With $A = \Pi r^2$ and:

$$P_m = \left(\rho \Pi r^2 V^3 C_p\right)/2 \tag{7}$$

If λ is the ratio between the blade tip speed to wind speed, then C_p becomes a function of λ. C_p relates to the pitch angle β (from rotor blade), and its theoretical upper limit is 0.59, according to the Betz limit. Hence:

$$\lambda = R\omega/V \tag{8}$$

And:

$$C_p = 0.5[116/\lambda_1 - (0.4B) - 5]Exp\{-16.5/\lambda_1\} \tag{9}$$

The wind turbine torque on the shaft is calculated from the power as follows:

$$T_m = P_m/\omega = \left(\rho \Pi r^2 V^3 C_p/2\omega\right) \tag{10}$$

If the tip speed ratio formula is employed, then the torque coefficient T_m is:

$$T_m = \left(\rho \Pi r^3 V^2 C_p/2\lambda\right) \tag{11}$$

Using the ratio of power coefficient to the tip speed ratio $C_t = C_p/\lambda$, it becomes:

$$T_m = \left(\rho \Pi r^3 V^2 C_t/2\lambda\right) \tag{12}$$

2.3 Control Strategy for Maximum Power Point Tracking (MPPT)

Although the wind speed changes with time, wind turbine optimization can run at near peak power production for several wind speeds. Besides output optimization, different control methods are applicable. Subsequently, the suggested control strategy is discussed.

The eolic turbine sends maximum power by altering the rotor speed consistent with the airstream speed to function at the leading power coefficient (C_p). The MPPT control is an active area undergoing an investigation to get maximum power from the existing wind power. The DC voltage measurements from both the three-phase diode bridge rectifier and the wind turbine power source during the DC-DC boost chopper's duty cycle control provide wind turbine MPPT. Figure 2 depicts a general relation between power and voltage, which resembles the mechanical energy and rotor speed of the PMSG relationship. The controller is developed with two inputs to reduce the error and number

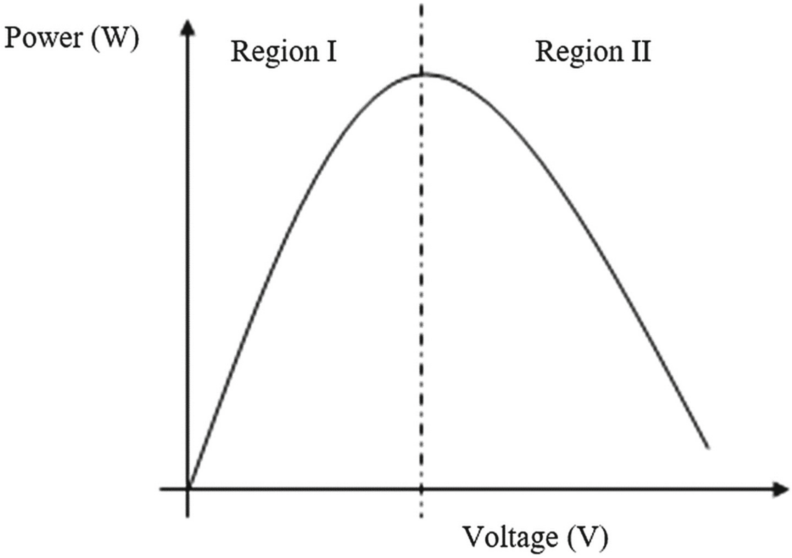

Fig. 2. Power vs. voltage curve

of the control blocks, which produces the right duty cycle to the boost chopper, with maximum output power. Figure 2 reveals one point corresponding to the full power at any wind speed value at a specific amount of DC voltage. The PMSG rotor speed and the DC voltage follow a linear relationship. They are changing the chopper duty ratio shifts the operating point from one curve to another with changing wind speed.

As indicated in Fig. 2, the power-voltage curve encompasses two regions:

1. Positive Region (located on the right side of the MPP).
2. Negative Region (located on the left side of the MPP).

Table 1. Control actions for various operating points

ΔP	+	+	−	−
ΔV	+	−	+	−
Region	**I**	**II**	**II**	**I**
ΔD	−	+	+	−

Table 1 condenses the control actions and describes the recommended MPPT procedure. The voltage varies as the wind speed changes. The boost chopper control goes periodically and aims at tracking the optimum operational point by sensing the turbine output power and output voltage of the rectifier by varying the duty ratio of the boost chopper according to the control strategy proposed.

2.4 Algorithm for the Maximum Power Point Tracking (MPPT) Using PWM (MPPT-PWM)

The MPPT Algorithm includes several steps summarized below:

1. First, the DC voltage at the rectifier and power of the wind turbine.
2. Then, the DC voltage at the wind turbine's rectifier and power in the $(K + 1)$ iteration.
3. Compare the previous wind turbine power, voltage value with new wind turbine power, voltage by using the formulae:

$$\Delta P = P(K + 1) - P(K) \tag{13}$$

And:

$$\Delta V = V(K + 1) - V(K) \tag{14}$$

4. Check whether $\Delta P > 0$ or $\Delta P < 0$. Based on the following four conditions duty ratio of the boost chopper is increased or decreased.

   - If $\Delta P > 0$ and $\Delta V > 0$, then $D = D - \Delta D$
   - If $\Delta P > 0$ and $\Delta V < 0$, then $D = D + \Delta D$
   - If $\Delta P < 0$ and $\Delta V < 0$, then $D = D - \Delta D$
   - If $\Delta P < 0$ and $\Delta V > 0$, then $D = D + \Delta D$

5. Repeat steps 3–5 until $\Delta P = 0$.

3 Results and Discussions

Several Matlab-Simulink simulations have been carried out to validate the design of the MPPT-PWM framework. They are depicted and analyzed subsequently.

3.1 Simulated Model for the WECS

MATLAB-Simulink Models. Figure 3 depicts the model that simulates the eolic turbine. The corresponding inputs are wind velocity, clock pulse, the turbine's angular velocity, the generator's angular velocity, and the stator voltage. The wind turbine outputs are the turbine's angular velocity, the generator's angular momentum, stator voltage, λ, power coefficient C_p, torque, and power.

Figure 4 shows the Matlab/Simulink model for the PMSG for different wind speeds with the permanent magnet generator's corresponding performance analysis. Figure 5 shows the WECS system simulation model that consists of a wind turbine, a PMSG, boost chopper with an inverter block undergoing simulations at various wind velocities. The wind turbine inputs are wind velocity, clock pulse, the turbine angular velocity, the generator's angular velocity, and the stator voltage.

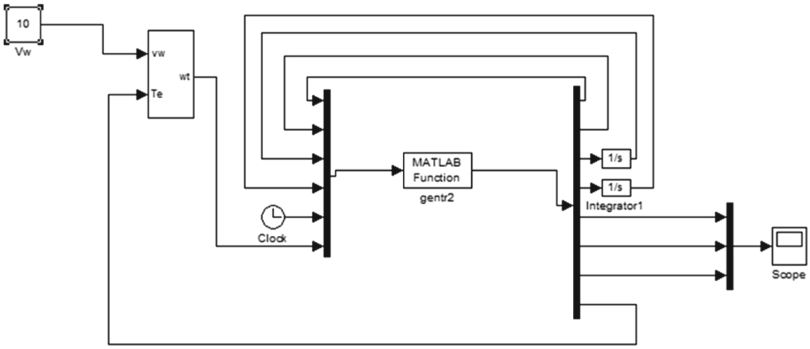

Fig. 3. Matlab/Simulink model for the wind turbine.

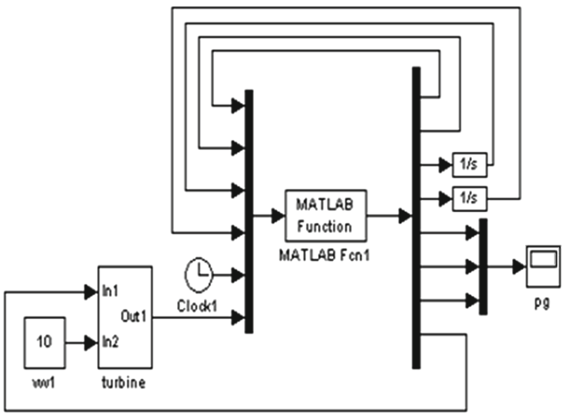

Fig. 4. Matlab/Simulink PMSG model.

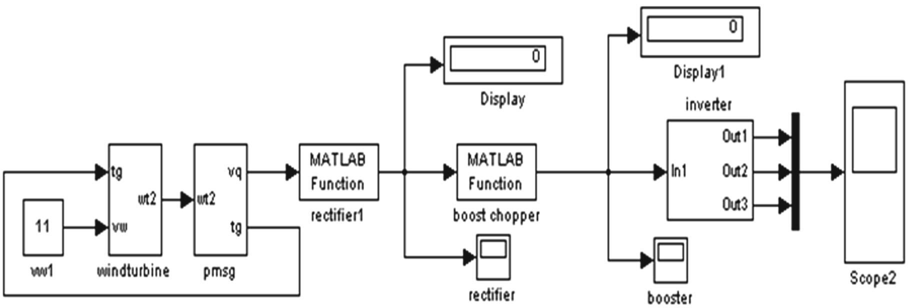

Fig. 5. Matlab/Simulink model for WECS.

Figure 6 shows the overall MPPT-PWM system simulation model, which comprises a wind turbine module, permanent magnet generator unit, boost chopper, inverter circuit, and control blocks. The controller output is duty-cycled. It is fed into the boost chopper.

Simulation entails various wind velocities and aid in performing analysis. The wind turbine receives the wind velocity, clock pulse, the turbine's angular velocity, the angular velocity of the generator, and the stator voltage.

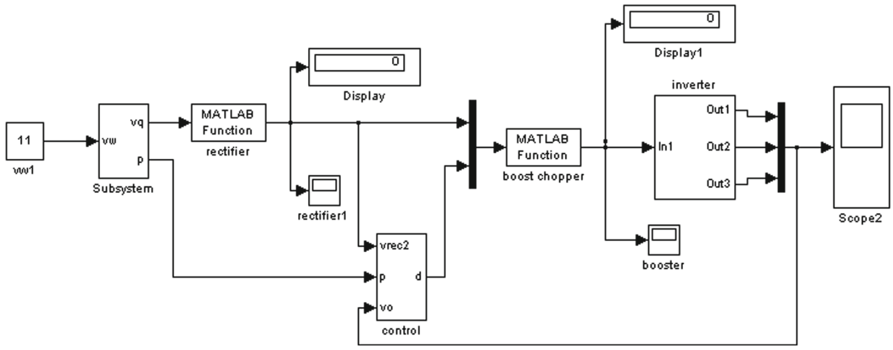

Fig. 6. Matlab/Simulink model for the overall MPPT-PWM system.

3.2 Power vs. Speed Characteristics

Figure 7 displays the Power vs. Speed characteristic curve of the eolic turbine. For example, with a wind velocity of 11 m/sec, then the equal power and speed values are 1241 W and 31 rpm, respectively. Likewise, the power vs. Speed characteristic curve is obtained for several wind speed values.

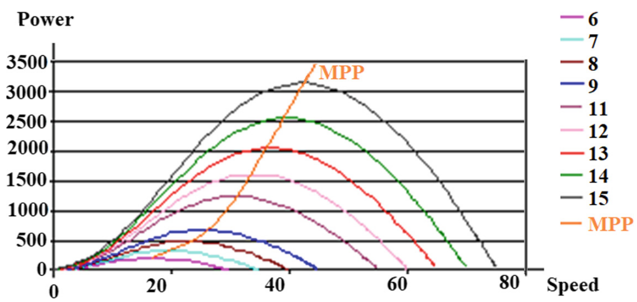

Fig. 7. Power vs. speed characteristics of the wind turbine.

PMSG Output Waveform. Figure 8 shows the PMSG output waveform, where for a 10 m/s wind velocity, the peak-to-peak voltage is 78 V. Increasing the wind velocity also augments the PMSG voltage.

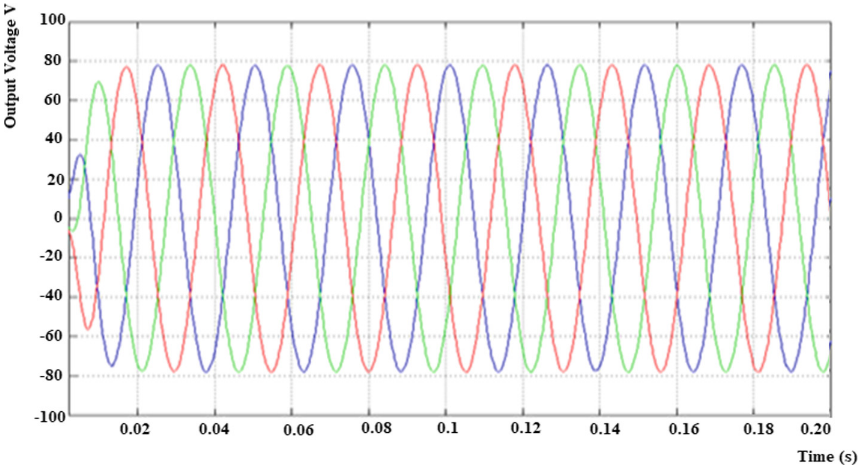

Fig. 8. PMSG output waveform

Figure 9 displays the diode rectifier output for a wind velocity of 10 m/s. This component transforms the AC voltage input into DC. The rectifier output goes to the boost chopper, where there is a control to maintain a constant voltage and peak power.

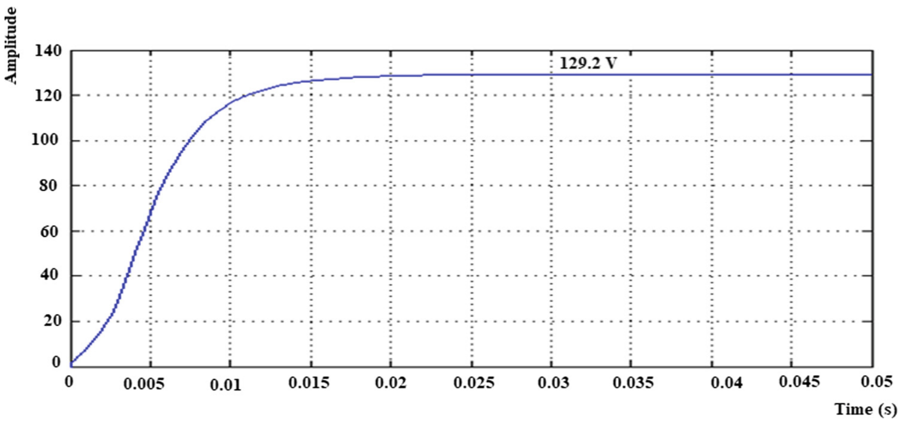

Fig. 9. Rectifier output voltage.

Inverter Output Voltage. Figure 10 depicts the inverter output voltage, which converts the incoming dc voltage into equivalent AC. The inverter is of a Sinusoidal Pulse Width Modulated (SPWM) type. The PWM pulses fed to the six inverter switches result from three-phase sinusoidal reference waves with a triangular carrier wave.

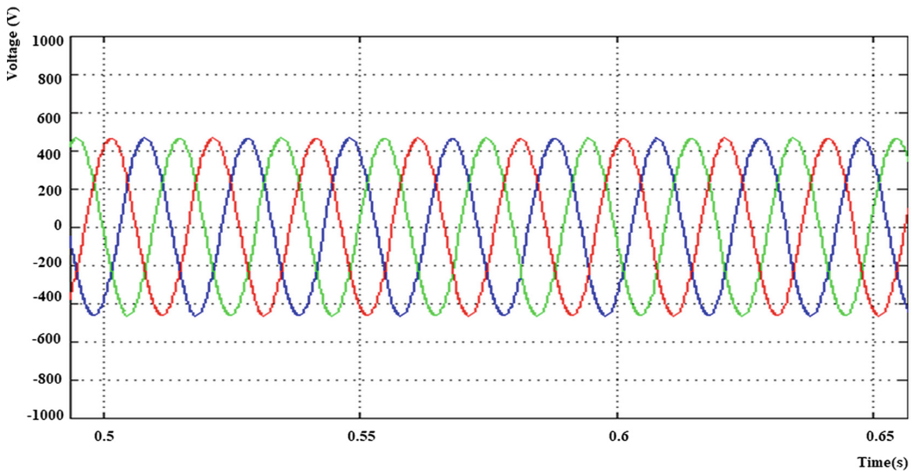

Fig. 10. Inverter output voltage.

4 Conclusion

This work introduces a system called MPPT-PWM for variable-speed wind energy transformation employing a PMSG within a grid with sustainable and clean energy sources. The optimal duty cycle control of the chopper delivered maximum power to the wind turbine. The rectifier output voltage is used as the reference for the MPPT control. Likewise, the MPPT control works without a wind speed sensor with a simple control algorithm (compared to other existing methodologies, which utilizes voltage and power as references). The MPPT-PWM method is advantageous since it is independent of information about wind velocity or optimal wind generator power characteristics.

Experiments using Simulink confirmed that the design's viability had been performed with suitable batteries and supercapacitors. Wind-based energy can benefit from decent charging time, charging efficiency, and energy system lifetime despite leakage and residual strength.

The future will have energy harvesters working with wireless communications. According to the demands and availability of alternative energy sources, transducers will transform non-electrical energy into electrical power. Radio-Frequency (RF) energy harvesters can convert using wind, photovoltaic cells, or other energy types [15]. They will demand models that predict the necessary amount of power, energy availability, and useful optimization algorithms to establish the optimum combination of energy sources and routing [16] straightforwardly.

References

1. Mitchell K, Nagrial M, Rizk J (2005) Simulation and optimization of renewable energy systems. Electr Power Energy Syst 27:177–188
2. Masserant BJ, Stuart TA (1997) Maximum power transfer battery charger for electric vehicles. IEEE Trans Aerosp Electron Syst 33(3):930–938

3. Thiagarajan Y, Shanmugasundaram APC (2007) Design and simulation of Pi controller for a DC-DC boost converter using renewable energy system. In Proceedings of AICTE sponsored 4th national control instrumentation system conference CISCON-2007. MIT
4. Hirakata M, Shimizu T, Kimura G (1996) Generation control circuit for a PV system. In: Proceedings of ICEE 1996, vol 2, pp 992–996
5. Thiagarajan Y, Kavitha BS (2011) Efficient voltage regulation for a standalone photovoltaic system using PI and fuzzy controller for AC voltage application. Int J Technol Eng Syst (IJTES) 2:3
6. Browny SB, Salameh ZM (1999) Optimum photovoltaic array size in a hybrid wind/PV system. IEEE Trans Energy Convers 9:3
7. Yip SC, Qiu D, Chung H, Hui SY (2003) A novel voltage sensorless control technique for a bidirectional AC/DC converter. IEEE Trans Power Electron 18:1346–1355
8. Chapman RN (1987) A simplified technique for designing least-cost standalone photovoltaic/storage systems. In: 19th IEEE photovoltaic specialists conference, pp 1117–1121
9. Chen YM, Liu YC, Hung SC, Cheng CS (2007) Multi-input inverter for grid-connected hybrid PV/wind power system. IEEE Trans Power Electron 22(3):1070–1077
10. Chinchilla M, Arnaltes S, Burgos JC (2006) Control of permanent-magnet generators applied to variable-speed wind-energy systems connected to the grid. IEEE Trans Energy Convers 21(1):130–135
11. Neammanee B, Krajangpan K, Sirisumrannukul S, Chatrattana S (2007) Maximum peak power tracking-based control algorithms with stall regulation for optimal wind energy capture, pp 1424–1430
12. Anandavel P, Rajambal K, Chellamuthu C (2005) Power optimization in a grid-connected wind energy conversion system. In: Proceedings of IEEE Conference on PEDS 2005, pp 1617–1621
13. Morimoto S, Nakayama H, Sanada M, Takeda Y (2005) Sensorless output maximization control for variable-speed wind generation system using IPMSG. IEEE Trans Ind Appl 41(1):60–67
14. Rashid MH (2001) Power electronics handbook. Academic Press
15. Razmjooy N, Khalilpour M, Estrela VV, Loschi HJ (2019) World Cup optimization algorithm: an application for optimal control of pitch angle in hybrid renewable PV/wind energy system. In: Quiroz M, et al (eds) Proceedings of NEO 2018: numerical and evolutionary optimization
16. Razmjooy N, Estrela VV, Loschi HJ, Farfan WS (2019) A comprehensive survey of new meta-heuristic algorithms. In: De S, Dey S, Bhattacharyya S (eds) Recent advances in hybrid metaheuristics for data clustering. Wiley Publishing